

*General-Purpose Heat Source:  
Research and Development Program*

*High-Silicon Fuel Characterization Study;  
Half Module Impact Tests 1 and 2*

RECEIVED  
APR 29 1996  
OSTI

MASTER

**Los Alamos**  
NATIONAL LABORATORY

*Los Alamos National Laboratory is operated by the University of California  
for the United States Department of Energy under contract W-7405-ENG-36.*

**DISTRIBUTION OF THIS DOCUMENT IS UNLIMITED**

*Edited by Jennifer Graham, CIC-1*

*This work was supported by the U.S. Department of Energy, Office of Nuclear Energy.*

*An Affirmative Action/Equal Opportunity Employer*

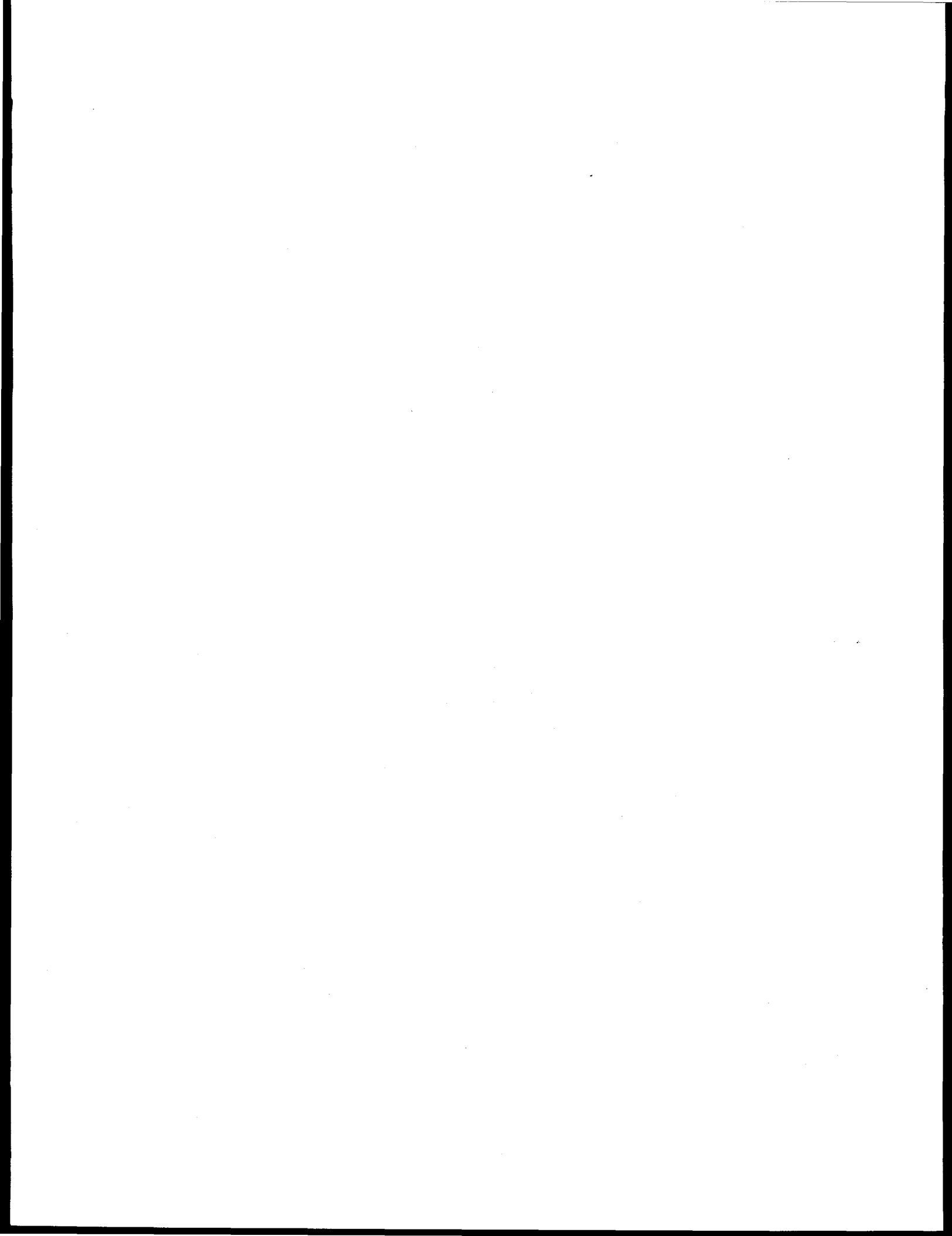
*This report was prepared as an account of work sponsored by an agency of the United States Government. Neither The Regents of the University of California, the United States Government nor any agency thereof, nor any of their employees, makes any warranty, express or implied, or assumes any legal liability or responsibility for the accuracy, completeness, or usefulness of any information, apparatus, product, or process disclosed, or represents that its use would not infringe privately owned rights. Reference herein to any specific commercial product, process, or service by trade name, trademark, manufacturer, or otherwise, does not necessarily constitute or imply its endorsement, recommendation, or favoring by The Regents of the University of California, the United States Government, or any agency thereof. The views and opinions of authors expressed herein do not necessarily state or reflect those of The Regents of the University of California, the United States Government, or any agency thereof. The Los Alamos National Laboratory strongly supports academic freedom and a researcher's right to publish therefore, the Laboratory as an institution does not endorse the viewpoint of a publication or guarantee its technical correctness*

*General-Purpose Heat Source:  
Research and Development Program*

*High-Silicon Fuel Characterization Study;  
Half Module Impact Tests 1 and 2*

*M. A. H. Reimus  
T. G. George*

**DISTRIBUTION OF THIS DOCUMENT IS UNLIMITED**



# **GENERAL-PURPOSE HEAT SOURCE: RESEARCH AND DEVELOPMENT PROGRAM**

High-Silicon Fuel Characterization Study;

Half Module Impact Tests 1 and 2

by

M. A. H. Reimus and T. G. George

## **ABSTRACT**

The General-Purpose Heat Source (GPHS) provides power for space missions by transmitting the heat of  $^{238}\text{Pu}$  decay to an array of thermoelectric elements. Because any space mission could experience a launch abort or return from orbit, the heat source must be designed and constructed to survive credible accident environments. Previous testing conducted in support of the Galileo and Ulysses missions documented the response of GPHSs to a variety of fragment-impact, aging, atmospheric reentry, and Earth-impact conditions. The evaluations documented in this report are part of an ongoing program to determine the effect of fuel impurities on the response of the heat source to conditions baselined during the Galileo/Ulysses test program. In the first two tests in this series, encapsulated GPHS fuel pellets containing high levels of silicon were aged, loaded into GPHS module halves, and impacted against steel plates. The results show no significant differences between the response of these capsules and the behavior of relatively low-silicon fuel pellets tested previously.

---

## **I. INTRODUCTION**

The General-Purpose Heat Source (GPHS) is a modular component of the radioisotope thermoelectric generators (RTGs) that provide power for the National Aeronautics and Space Administration's (NASA's) planetary exploration missions. An RTG generates electric power by using the heat of  $^{238}\text{Pu}$   $\alpha$ -decay to create a temperature differential across a thermoelectric array. Each RTG is loaded with 18 GPHS modules, and each GPHS module (Fig. 1) contains four  $^{238}\text{PuO}_2$  fuel pellets that provide a total thermal output of

250 W. Each fuel pellet is encapsulated in a vented, DOP-26 iridium alloy shell. Two capsules are held in a Fineweave-Pierced Fabric\* (FWPF) graphite impact shell (GIS), and two GISs are contained within an FWPF aeroshell.

Because any space mission could experience a launch abort or return from orbit, the GPHS has been designed and constructed to survive credible accident environments. Previous testing conducted in support of the Galileo and Ulysses missions documented the response of the GPHS heat source to a variety of fragment-impact, aging, atmospheric reentry, and Earth impact conditions.<sup>1-4</sup> The tests described in this report are part of an ongoing program to determine the effect of fuel impurities on the response of the heat source to conditions baselined during the Galileo/Ulysses test program. In the first two tests in this series, encapsulated GPHS fuel pellets containing high levels of silicon were aged, loaded into GPHS module halves, and impacted against steel plates at 970°C and a nominal velocity of 55 m/s.

## II. BACKGROUND

Four fuel pellets encapsulated at Los Alamos National Laboratory (LANL) in 1993 and 1994 were selected for use in the first two half module impact tests in the High-Silicon Fuel Characterization Study. The two pellets selected for the first test, HSC-1, were fabricated from low-enrichment (<82%  $^{238}\text{Pu}$ ) fuel and contained relatively high concentrations of silicon (>1000 ppm). The GPHS capsules containing these pellets were loaded into a GIS (designated as GIS A), which was then paired with another GIS (designated as B) and loaded into a GPHS module. A third GIS (designated as GIS D) was loaded with GPHS capsules that contained fuel pellets with silicon levels of 415 and 605 ppm. This GIS was paired with GIS C and loaded into a second GPHS module.

We treated both GPHS modules in a module reduction and monitoring facility (MRMF) furnace system. Each module was loaded into a stainless steel box fabricated from thin sheet. The module was insulated with approximately 50 mm of outgassed graphite felt insulation and the box was then placed in a Centorr vacuum furnace; the furnace was evacuated and then backfilled with argon to a pressure of approximately 2 in. of Hg above atmospheric pressure. The temperature of each module during the MRMF treatment remained at a constant temperature; the first module (which contained GIS A) stabilized at a temperature of 920°C, and the second module stabilized at 862°C. Samples of the furnace chamber atmosphere were periodically taken and analyzed with high resolution mass spectrometry for CO and  $\text{CO}_2$  partial pressure. This data were used to calculate the  $\text{PuO}_x$  stoichiometry of the fuel. The MRMF treatment was continued until a fuel stoichiometry of approximately 1.98 O/Pu was reached.

After MRMF treatment, each module was soaked at 1074°C in vacuum ( $5 \times 10^{-7}$  torr) for an extended time period; this treatment temperature had been calculated to give a fuel temperature of 1461°C. After the aging treatment, the modules were removed from the furnaces, and GISs A and D were loaded into half GPHS modules for impact testing. The GIS loadings, calculated pellet silicon contents, and heat treatment schedules are listed in Table I.

---

\* Fineweave-Pierced Fabric 3-D carbon/carbon composite, a product of AVCO Systems Division, 201 Lowell St., Wilmington, MA 01887.

Table I. History and Treatment Schedule For High-Silicon Characterization Study Test Components

GIS No.	MRMF		Post-MRMF Treatment at 1074°C <sup>a</sup>	GPHS Capsule No.	Fuel Pellet No.
	Treatment Duration (days)				
A	98		200 hours	FC0007 FC0010	GQ-02 GQ-04
D	55		108 days	FC0033 FC0035	GF-20 GF-22

<sup>a</sup>This treatment temperature has been calculated to give a fuel temperature of 1461°C.

### III. EXPERIMENTAL PROCEDURES

#### A. Impact Testing

After heat treatment, each GIS was placed in a graphite half module that had 50 mils removed from the exterior surfaces to simulate ablation. Thermocouple holes were drilled into the half module and GIS; a split-junction, Chromel-Alumel thermocouple was installed with its legs contacting one GPHS capsule. The position of the capsules in each GIS and the post-impact containment shell (PICS) number of the iridium components are listed in Table II.

Table II. History and Treatment Schedule For High-Silicon Characterization Study Test Components

GIS No.	GPHS Capsule No.	Location In GIS	PICS <sup>a</sup> No.	Max. Ultrasonic
				Test Rating (equiv. mils)
A	FC0007	Blind End	9808-00-1529	5.2
	FC0010	Open End	9808-01-2053	3.0
D	FC0035	Blind End	9808-01-2255	2.8
	FC0033	Open End	9808-01-2253	2.6

<sup>a</sup>Post-impact containment shell.

After loading, each half module was impacted in the Los Alamos Isotope Fuels Impact Test Facility (IFIT)<sup>4</sup> against a hardened steel target at 970°C and a nominal velocity of 55 m/s. The specific conditions for each test are listed in Table III.

Table III. High-Silicon Characterization Impact Test Parameters

Test	Module Orientation	Temp (°C)	Velocity (m/s)
HSC-1	Side-On	970	54.8±0.3
HSC-2	Side-On	970	54.4±0.2

### B. Postmortem Examination

The principle objectives of the postmortem examination were to document the macroscopic damage sustained by test components, determine the quantity of plutonia release (if any), and characterize the iridium and plutonia impact responses.

After each impact test, the impacted module (contained within a sealed catch tube) was transferred to LANL's plutonium Facility (building PF-4) and opened in a material-introduction hood. All test components were photographed and the fueled clads were measured to determine the post-impact capsule strains. The size and location of all clad failures and cracks were recorded.

After macroscopic examination, the fueled clads were opened and the patterns of fuel fracture were photographed. The clads were then defueled and samples of the fuel taken for chemical analysis and ceramographic examination. Each sample was carefully weighed and sized with certified sieves. The fuel was then submitted for particle size analysis. Any deposits or anomalies observed on the fuel, iridium clad, or graphite components were photographed. Samples of deposits were taken and submitted for chemical analysis.

The iridium clads were also sampled to provide specimens for metallographic analysis. At a minimum, the following metallographic sections were taken from each clad: axial and transverse sections of the vent and shield cup walls, vent cross section, and cross sections of single-pass weld and weld overlap regions. All clad failures and areas of severe localized deformation were sectioned for metallographic examination.

### IV. RESULTS

Results of the individual postmortem examinations are summarized in the following sections. Analytical data that resulted from these examinations are tabulated as follows:

- Table IV. HSC Capsule Strains
- Table V. HSC Iridium Grain Sizes
- Table VI. Particle Size Analyses, HSC Test Series
- Table VII. Fuel Impurity Analyses, HSC Test Series

Table IV. HSC Capsule Strains<sup>a</sup>

Test No.	GPHS Clad No.	GIS Location	Calculated Strains (%) <sup>a</sup>					
			Diametral					
			Vent Cup		Shield Cup		Axial	
			Max.	Min.	Max.	Min.		
HSC-1	FC0007	Blind End	+ 17.0	+ 2.7	+ 6.5	- 5.4	+ 4.0	
	FC0010	Open End	+ 18.4	- 0.3	+19.1	- 0.5	+10.8	
HSC-2	FC0035	Blind End	+ 10.7	- 7.6	+ 8.7	- 9.5	+ 5.8	
	FC0033	Open End	+ 6.5	- 3.8	+ 4.4	- 4.4	+ 4.0	

<sup>a</sup>Calculated on the basis of nominal pretest capsule dimensions (1.181 in. length.; 1.167 in. diam).

### A. HSC-1

The half module was impacted on a steel target at 54.8 m/s and 970°C. The impact orientation was side on, with the edge having the flight bevels leading. Upon opening the inner catch tube (ICT), no detectable amounts of contamination were found on the ICT lid, ICT interior, or outer surface of the module. There was no detectable deformation of the steel target. The module was relatively intact (Fig. 2), with a large crack on the impact face. The opposite face of the module was not cracked, but the cover for the GIS cavity had been dislodged.

The GIS was intact and had a small crack on the cap. Alpha counting of the GIS interior revealed a contamination level of approximately 15,000 counts per minute (cpm). There was no evidence of any deposits on the GIS interior or of pitting in the floating membrane between the two GPHS capsules. Both fueled clads were moderately deformed (Figs. 3 and 4), with FC0010 having the most deformation. The impact face of FC0007 was centered at approximately 345 deg (angular location is referenced clockwise from the weld start at 0 deg). The impact face of FC0010 was centered at approximately 90 deg. There were no visible cracks on the exterior of the clads and no evidence of fuel release. Smear surveys of the exterior surfaces of both capsules did not reveal any removable contamination.

When the fueled clads were opened, a thin coating of white powder was observed on both capsule interiors (Figs. 5 and 6). The deposits tended to be most pronounced at the vent ends of the capsules but were observed to a lesser degree on all interior surfaces. A white deposit, identical in appearance to the deposit on the capsule interiors, was also observed on the exterior of the fuel pellet recovered from FC0007 (Fig. 7). The deposits on the capsule interiors did not tightly adhere and were easily scraped from the surface. Samples of the deposits were taken and submitted for chemical analysis by electron microprobe analysis.

Table V. HSC Iridium Grain Size

Test No.	GPHS Clad No.	Iridium Cup No.	Average Grains/ 0.65-mm Wall <sup>a</sup>		Comments
			Transverse	Axial	
HSC-1	FC0007	9753-01-1811	NS <sup>b</sup>	19	Typical microstructure.
		3625-00-2350	NS	18	Typical microstructure.
HSC-1	FC0010	9753-01-1991	NS	21	Typical microstructure.
		3625-00-2350	NS	21	Typical microstructure.
HSC-2	FC0033	9753-01-3049	NS	20	Typical microstructure.
		3625-01-3013	NS	18	Typical microstructure. Slight coarsening on exterior surface.
HSC-2	FC0035	9753-01-3030	15	NS	Isolated coarse grains on interior and exterior surfaces. Pronounced grain growth at vent cover welds.
		3625-01-3533	14	17	Typical microstructure.

<sup>a</sup>The number of grains/wall thickness has been normalized to a nominal thickness of 0.65 mm.

<sup>b</sup>Not submitted for evaluation.

Because the fuel had a high silicon impurity level relative to the silicon specification of 200 ppm, the deposits on the capsule interiors were suspected being  $\text{SiO}_2$ . This premise was based on the volatility of  $\text{SiO}_2$  at the temperatures experienced by these fueled clads and on the appearance of the deposits. The results of the electron microprobe analyses indicated that the deposits were in fact  $\text{SiO}_2$  with small amounts of Ti, Fe, and Pu.

Examination of the as-opened FC0007 fuel capsule revealed the pattern of fuel breakup (Fig. 8). The fuel tended to fragment outward in a radial pattern from the point of initial impact.

Five sections were cut from the iridium shell of capsule FC0007 and four sections were cut from FC0010. All nine sections were mounted in epoxy and prepared for metallography. Examination of cross sections from both capsule vents did not reveal any deposits or anomalous microstructures in the vent frits or orifices (Fig. 9). However, there was a thin layer of discoloration on the interior surface (fuel side) of the vent assemblies. The discolored layers on the interior of the FC0007 and FC0010 vents were approximately 30 and 20  $\mu\text{m}$  thick, respectively.

The microstructures of the single-pass and weld overlap regions in both capsules were typical. Although some large grains were observed throughout the capsule walls, the microstructures appeared normal.

Microscopic examination of a sample removed from fuel pellet GQ-02 (originally loaded in capsule FC0007) revealed a typical plutonia microstructure (Fig. 10) with no obvious evidence of additional phases, intergranular deposits, or other anomalies. A fuel sample removed from pellet GQ-04 (originally loaded in capsule FC0010) was also submitted for examination. However, this fuel sample was unaffected by the standard etchant (93% HBr, 5% HCl, 2% HF) during the normal 8 h etch cycle, and in fact, remained unetched even after a 24 h treatment. The as-polished appearance of the sample was normal (Fig. 11).

## B. HSC-2

The half module was impacted on a steel target at 54.4 m/s and 970°C. The impact orientation was side on, with the edge having the flight bevels leading. The interior of the ICT was found to be contaminated during disassembly. Consequently, the ICT was introduced into the glovebox line and opened. There was no detectable deformation of the steel target.

Macroscopic examination revealed that the module was relatively intact (Fig. 12), with longitudinal cracks on the impact and opposite faces. The cap of the GIS cavity was dislodged during impact, but the GIS remained inside the module. The GIS was intact (Fig. 13), with several longitudinal cracks on the impact face.

The floating membrane between the two GPHS capsules apparently shattered during impact. Visual inspection of the largest pieces revealed no anomalies, deposits, or pitting of the graphite surface. Although the membrane surface was smooth on both sides, there were some small depressions that possibly were caused by impact of the GPHSs.

**1. FC0033.** GPHS capsule FC0033, which was loaded in the open end of the GIS was moderately deformed. Its impact face was centered at approximately 0 deg. No cracks or clad breaches were observed (Fig. 14). The vent area of the clad was clean, with no evidence of deposits or other foreign material. There was slight discoloration centered around the vent hole on the exterior of the capsule.

After macroscopic examination, capsule FC0033 was defueled. Examination of fuel pellet GF-20 did not reveal any deposits, coatings, or unusual features. Similarly, the interior of capsule FC0033 was free of any deposits and coatings.

Table VI. Particle Size Analyses, HSC Test Series

Particle Size Range ( $\mu\text{m}$ )	HSC-1		HSC-2	
	FC007	FC0010	FC0033	FC0035 <sup>a</sup>
+ 5600	0.1929	0.2055	0.3829	0.3212
+ 2000 to 5600	0.3210	0.3513	0.3866	0.3758
+ 850 to 2000	0.2989	0.2545	0.1570	0.1941
+ 425 to 850	0.1016	0.0957	0.0402	0.0617
+ 180 to 425	0.0525	0.0543	0.0178	0.0286
+ 125 to 180	0.0098	0.0113	0.0036	0.0055
+ 75 to 125	0.0094	0.0091	0.0037	0.0048
+ 45 to 75	0.0067	0.0070	0.0026	0.0031
+ 30 to 45	0.0004	0.0010	0.0005	0.0005
+ 20 to 30	0.0006	0.0019	0.0011	0.0007
+ 10 to 20	0.0012	0.0026	0.0019	0.0014
+ 9 to 10	0.0002	0.0004	0.0002	0.0002
+ 8 to 9	0.0002	0.0005	0.0001	0.0002
+ 7 to 8	0.0002	0.0005	0.0002	0.0002
+ 6 to 7	0.0005	0.0008	0.0002	0.0003
+ 5 to 6	0.0007	0.0009	0.0003	0.0003
+ 4 to 5	0.0009	0.0008	0.0003	0.0004
+ 3 to 4	0.0009	0.0007	0.0004	0.0003
+ 2 to 3	0.0004	0.0004	0.0002	0.0002
+ 1 to 2	0.0008	0.0006	0.0002	0.0004
$\leq 1$	0.0002	0.0002	0.0000	0.0001
Total:	1.0000	1.0000	1.0000	1.0000
Weight fraction $<10 \mu\text{m}$ :	0.0050	0.0058	0.0021	0.0020

<sup>a</sup>Particle size analysis was performed on 146.423 g of fuel retained in capsule FC0035.

Metallographic examination of a section from the FC0033 vent revealed typical microstructure. No evidence of foreign material or deposits was found in the vent frit or orifices. A nonbreaching crack was observed in an axial section removed from the impact face of the vent cup. This crack was exclusively intergranular and penetrated approximately 66% of the capsule wall.

The microstructures of the single-pass and weld overlap regions in capsule FC0033 were typical, as were the microstructures of the cup walls. Average grain sizes are listed in Table V.

A sample was removed from fuel pellet GF-20 and submitted for ceramography. Examination of the as-polished surface (Fig. 15) did not reveal any unusual features. However, this fuel sample was unaffected by the standard etchant during the normal 8 h etch cycle.

**2. FC0035.** GPHS capsule FC0035, which was loaded in the blind end of the GIS, was wedged firmly in the GIS and was difficult to remove. The GIS had to be cut before the capsule could be removed.

The impact face of capsule FC0035 was centered at approximately 90 deg from the weld start (Fig. 16). Three axial breaching cracks were observed on the impact face. One crack transected the weld but appeared to have been initiated outside the weld in the shield cup. This crack had an approximate length of 15.1 mm and a maximum width of 0.56 mm. Another crack was located on the vent cup; this crack had a length of 12.6 mm and a maximum width of 1.37 mm. A hairline crack that was located on the shield cup had a length of 39.1 mm. All of these cracks on the impact face were on, or in close proximity to, a ridge that had apparently been caused by the differential displacement of fuel pellet fragments. Examination of the GIS impact face at a location corresponding to the position of FC0035 revealed an indentation on the interior of the GIS. This indentation suggested that the damage to the clad in the ridge area was not caused externally.

Examination of the trailing face of capsule FC0035 also revealed a large breaching crack that extended from the top of the vent cup to the shield cup radius (approx. 30 mm) and had a maximum width of 1.88 mm. The crack was located directly opposite the axial ridge noted on the impact face of the capsule. A weld centerline crack intersected and was apparently initiated by the displacement associated with the large axial crack. The weld centerline crack had an approximate length of 18.8 mm, and a maximum width of 0.7 mm.

After macroscopic examination, capsule FC0035 was defueled. The fuel removed from the capsule was weighed, and it was determined that a total of 3.684 g of plutonia had been released. Examination of the remains of fuel pellet GF-22 did not reveal any deposits or unusual features. Similarly, the interior of capsule FC0035 was free of any deposits and coatings.

Numerous sections for metallographic examination were removed from capsule FC0035. Pronounced grain coarsening was observed in a vent cup section, below and adjacent to the vent cover welds (Fig. 17). Although the wall adjacent to one of the welds contained only two grains/thickness, the coarsening effect was localized and did not appear to have affected other regions of the iridium clad. The remainder of the vent cup, as well as the shield cup, had typical microstructures. Unfortunately, during metallographic preparation of the cross section that contained the FC0035 vent, the central vent structures were destroyed and it was not possible to microscopically examine the vent frit or orifices.

Examination of wall sections that contained the major breach on the trailing face of the capsule did not reveal any unusual features. The fracture (Fig. 18) was exclusively intergranular, with slight grain deformation and wall thickness reduction. There were no microstructural indications to suggest that the breach was caused by anything other than a fuel fragment push-through.

Similarly, examination of the centerline weld failure that extended from the breaching crack did not reveal any unusual features. Although the weld microstructure in this region was somewhat coarse (Fig. 19), it was still acceptable, with numerous grains across the wall thickness. As in the case of the main breach, there were no indications that the failure was related to anything other than the relatively large differential displacement associated with the fuel fragment push-through.

Table VII. Fuel Impurity Analyses, HSC Test Series

Element & Spec. Limit (ppm)	Impurity Level (ppm)								
	HSC-1		HSC-2		GQ-02		GQ-04		
	Calc. <sup>a</sup>	Actual <sup>b</sup>	Calc.	Actual	Calc.	Actual	Calc.	Actual	
Al	150	191	145	47	130	69	83	30	90
B	15	31	<5	13	<5	5	<5	9	<5
Be	15	1	<1	1	<1	1	<1	1	<1
Ca	300	82	4	123	48	6	31	5	36
Cd	50	10	<10	10	<10	10	<10	10	<10
Cr	250	217	555	172	375	98	98	84	120
Cu	100	19	<1	29	<1	14	<1	55	<1
Fe	800	674	435	581	455	234	63	234	93
Mg	50	33	52	45	50	50	11	21	16
Mn	50	15	47	35	35	9	6	11	8
Mo	250	20	<20	20	<20	20	<20	54	<20
Na	250	56	<50	55	<50	50	<50	50	<50
Ni	150	82	31	75	16	46	6	76	5
P	25	13	ND <sup>c</sup>	19	ND	22	ND	20	ND
Pb	100	19	<10	46	<10	16	<10	13	<10
Si	200	905	1500	1059	1260	415	735	605	760
Sn	50	5	<5	5	<5	5	<5	5	<5
Zn	50	20	<5	10	<5	8	<5	5	<5
Total	≤2855	2393	2876	2345	2476	1078	1140	1288	1235

<sup>a</sup> Calculated on the basis of analyses of fuel lots used to fabricate the pellet.

<sup>b</sup> Based on analyses of fuel pellet samples.

<sup>c</sup> Not determined; phosphorus analyses are not routinely performed on fuel granules used to fabricate pellets.

Examination of the cracks on the impact face of capsule FC0035 did not reveal any anomalies. All of the wall sections adjacent to these cracks were relatively fine-grained and free of microstructural anomalies. The cracks appeared to be typical of iridium failures observed in other module impacts. All of the cracks were exclusively intergranular (Fig. 20).

A sample was removed from fuel pellet GF-22 and submitted for ceramography. Examination of the as-polished and etched surfaces (Fig. 21) did not reveal any unusual features. However, this fuel sample was unaffected by the standard etchant during the normal 8 h etch cycle; a total etching time of 24 h was required before the grain boundaries of the sample became clearly defined.

## V. DISCUSSION

### A. Fueled Clad Impact Response

The impact response of the capsules used in the first two HSC tests can best be summarized as contradictory. The capsules used in HSC-1 survived levels of deformation that far exceeded the strains reported for capsules tested to failure in similar safety

verification test (SVT) and design iteration test (DIT) impact tests.<sup>2-9</sup> Conversely, in HSC-2, nearly identical impact conditions produced an extensive failure of capsule FC0035 and capsule strains similar to those observed in the SVT and DIT test series. Further, there were no apparent anomalies in the impact responses of the HSC fuel pellets that could be directly associated with the large differences in capsule deformation.

It should be noted, however, that the fuel pellets used in the HSC tests were relatively young in relation to the pellets used in the DIT and SVT test series. Static pellet degradation and loss of integrity appear to be related to both age and thermal stress. In addition, localized strains that occur as a result of the differential displacement of sharp fuel fragments have been documented as the predominant failure mechanism for impacted GPHS capsules. Therefore, it may be that the impact responses of capsules used in previous test series were more a reflection of the degree of pellet fragmentation than an indicator of intrinsic fuel or cladding strength.

Extension of this hypothesis to the behavior of capsules tested in the HSC tests would provide an explanation for the apparent anomalies in capsule deformation and failure. FC0035 breached as a result of massive fuel fragment displacement and was the sole capsule tested in these two impacts that had been loaded with a nonintegral fuel pellet (pellet GF-22 was in four pieces at the time of capsule loading). In addition, as opposed to the capsules and fuel pellets evaluated in the DIT and SVT test series, none of the HSC capsules were subjected to additional stresses such as flight-acceptance vibration, cross-country shipment, and long-term storage that would be expected to accelerate fuel pellet degradation. Further, the capsules used in HSC-2 were aged at temperature for nearly thirteen times as long as were the capsules tested in HSC-1; both capsules used in the second test had deformations similar to those observed in the SVT and DIT test series.

If the extent of pretest pellet breakup is indeed an indicator of impact response, it would seem prudent to radiograph each GPHS capsule selected for evaluation immediately before testing. This was the standard practice for capsules tested in the DIT and SVT series.

Another potential explanation for the unusually high capsule strains observed in HSC-1 may be that the silica coating observed in both capsules effectively lubricated the surface of the iridium clad, thereby producing a more favorable strain state as the metal was deformed by the displacement of large fuel fragments. If this was the case, the deformations observed in the HSC-1 capsules may represent the effective limit of capsule strain that can be achieved without loss of containment.

## B. Fuel Chemistry

Comparison of the calculated and as-analyzed fuel chemistries did not reveal any clear trends. The as-analyzed aluminum contents were generally somewhat higher than the predicted values, but in one pellet (GQ-02) the aluminum content was slightly lower than expected. All of the variations between calculated and analyzed aluminum contents were relatively small and were within the band of possible analytical variance. In addition, all of the as-analyzed aluminum contents were less than the specification limit of 150 ppm.

The as-analyzed iron and nickel contents of the fuel pellets were constantly lower than the calculated values and considerably below specification limits (800 and 150 ppm, respectively). Interestingly, three of the as-analyzed chromium contents were higher than the calculated values.

All of the as-analyzed silicon levels were higher than the predicted values. The increases ranged from 19% to 77%. All of the differences between calculated and as-analyzed silicon values were within the range of possible analytical variance and may not represent real differences in chemical composition. However, the silica layers observed on the interiors of the HSC-1 capsules suggest that the silicon contents of these pellets were even higher at the time of encapsulation.

### C. Impurity Effects

No anomalous or detrimental conditions were observed in the capsules used in these tests that could be correlated with the relatively high impurity contents of the plutonia fuel pellets. There was no evidence of vent plugging, of formation and deposition of intermetallic compounds, or of intergranular attack of the iridium cladding. Although the interior surfaces of the HSC-1 capsules were coated with a layer of silica, there was no evidence that this coating was in any way detrimental to the aging or impact response of these capsules. On the contrary, and as previously discussed, the silica coatings may have enhanced the impact response of the capsules.

It should be noted, however, that none of the capsules evaluated in these tests were subjected to factors such as reentry heating that could favor greater mobilization of fuel impurities, or more extensive reactions with the iridium cladding.

### D. Particle Size Analyses

The results of particle size analyses of the four fueled clads tested in HSC-1 and HSC-2 indicate that pellet breakup and fragmentation are similar to those observed in capsules tested in the SVT series conducted at LANL in the mid 1980s.<sup>2-4</sup> The  $\leq 10 \mu\text{m}$  weight fraction of the fuel in all three unbreached capsules (FC0007, FC0010, FC0033) was within the range of  $\leq 10 \mu\text{m}$  weight fractions observed in the 13 SVT impact tests. However, it should be noted that the capsules tested in the SVT series were subjected to two cycles of flight-acceptance vibration spectra and transient accelerations, a reentry heating simulation at temperatures up to approximately 1580°C, and vibration and transient accelerations associated with cross-country shipping. The potential effect of these pretreatments on pellet breakup and  $\leq 10 \mu\text{m}$  fines generation is unknown.

## VI. CONCLUSIONS

1. The relatively high silicon contents of the fuel pellets used in the first two HSC tests did not appear to have any quantifiable effect on impact response, vent function, or iridium microstructure.
2. The sole failure observed in the first two HSC impact tests was apparently caused by differential displacement of a large fuel fragment.
3. The fines generation observed in the HSC-1 and HSC-2 was similar to that observed in the SVT series.

## VII. RECOMMENDATIONS

All GPHS capsules selected for impact testing should be radiographed immediately before testing.

## ACKNOWLEDGMENTS

We thank G. Rinehart for treating the GPHS capsules used in this study; C. Frantz, A. Herrera, and W. Bast for conducting the impact tests; T. Baros, E. Burciaga, C. Lynch, P. Moniz, and M. Padilla for doing metallography, sample preparation, and particle size analyses; W. Hutchinson for performing microprobe analyses, and J. Olivares and C. Collier for performing fuel spectrochemical analyses.

## REFERENCES

1. T. A. Cull and D. Pavone, "General-Purpose Heat Source Development: Safety Verification Test Program; Flyer Plate Test Series," Los Alamos National Laboratory report LA-10742-MS (September 1986).
2. D. Pavone, T. G. George, and C. E. Frantz, "General-Purpose Heat Source Safety Verification Test Series: SVT-1 Through SVT-6," Los Alamos National Laboratory report LA-10353-MS (June 1985).
3. T. G. George and D. Pavone, "General-Purpose Heat Source Safety Verification Test Series: SVT-7 Through SVT-10," Los Alamos National Laboratory report LA-10408-MS (September 1985).
4. T. G. George and D. Pavone, "General-Purpose Heat Source Safety Verification Test Series: SVT-11 Through SVT-13," Los Alamos National Laboratory report LA-10710-MS (May 1986).
5. F. W. Schonfeld, "General-Purpose Heat Source Development: Safety Test Program, Postimpact Evaluation, Design iteration Test 1," Los Alamos National Laboratory report LA-9680-SR (April 1984).
6. F. W. Schonfeld and T. G. George, "General-Purpose Heat Source Development: Safety Test Program, Postimpact Evaluation, Design iteration Test 2," Los Alamos National Laboratory report LA-10012-SR (June 1984).
7. F. W. Schonfeld and T. G. George, "General-Purpose Heat Source Development: Safety Test Program, Postimpact Evaluation, Design iteration Test 3," Los Alamos National Laboratory report LA-10034-SR (July 1984).
8. T. G. George and F. W. Schonfeld, "General-Purpose Heat Source Development: Safety Test Program, Postimpact Evaluation, Design iteration Test 4," Los Alamos National Laboratory report LA-10217-SR (December 1984).
9. T. G. George and F. W. Schonfeld, "General-Purpose Heat Source Development: Safety Test Program, Postimpact Evaluation, Design iteration Test 5," Los Alamos National Laboratory report LA-10232-SR (December 1984).

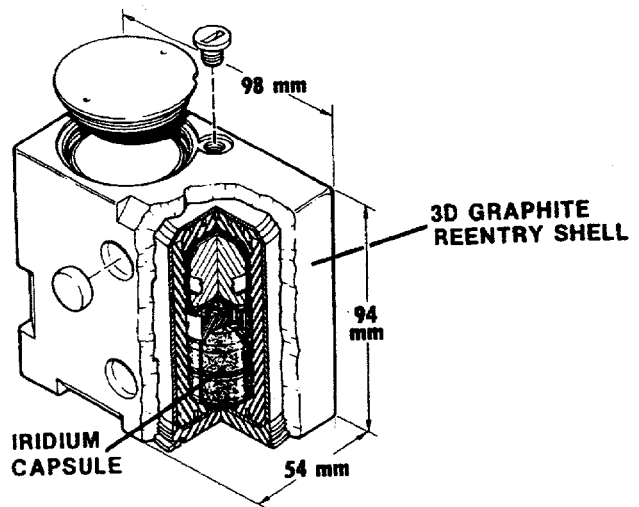


Fig. 1. The GPHS Module.

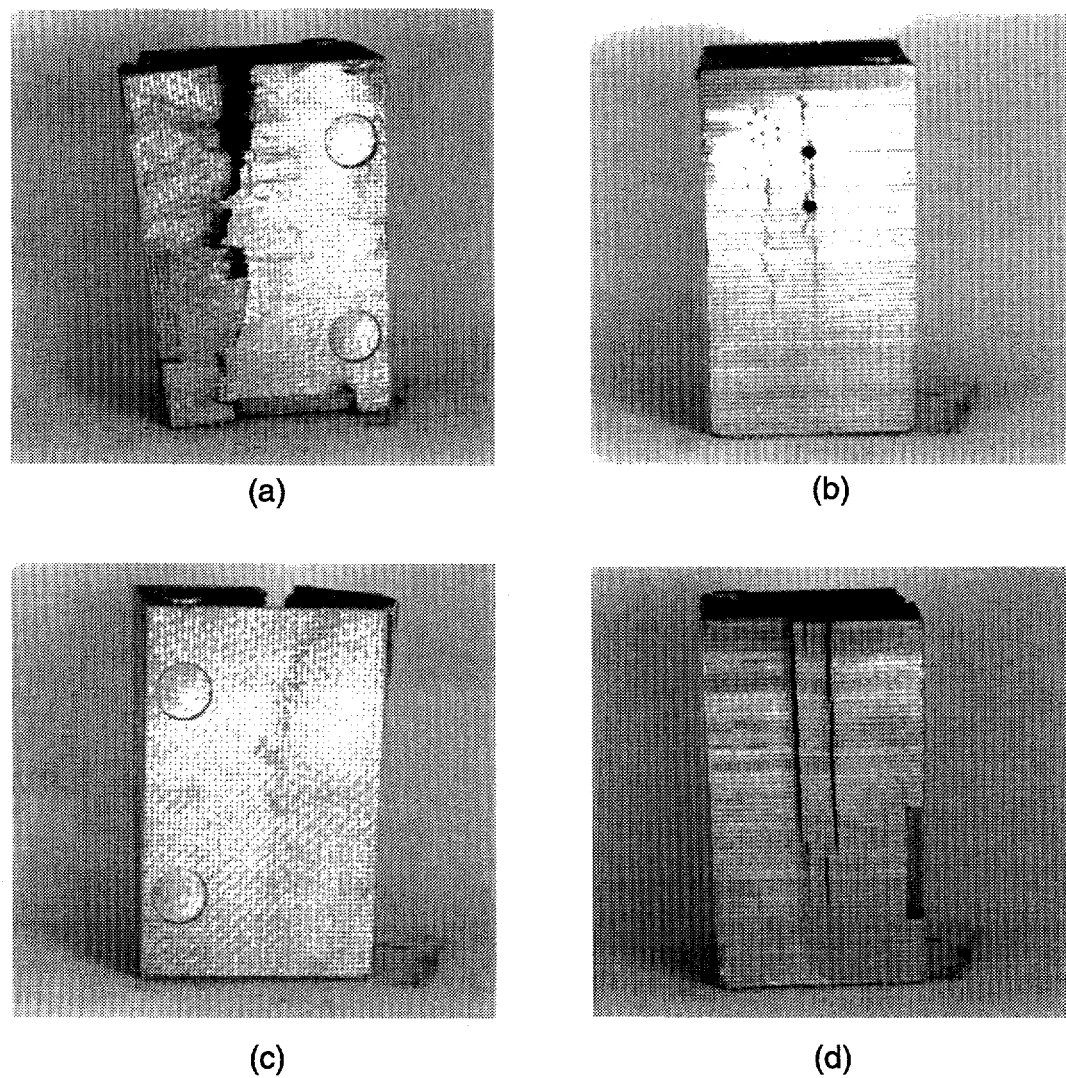
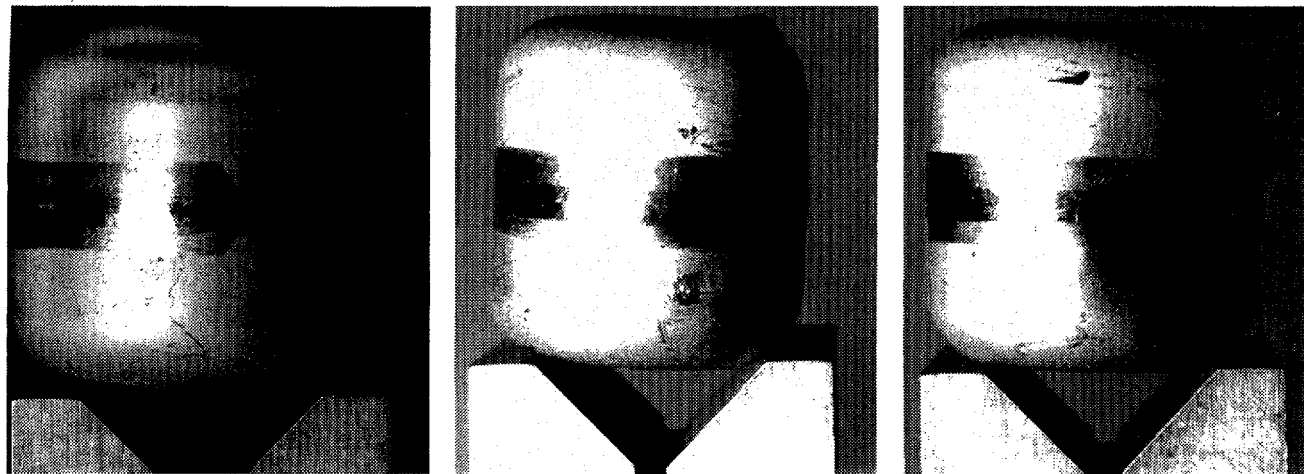


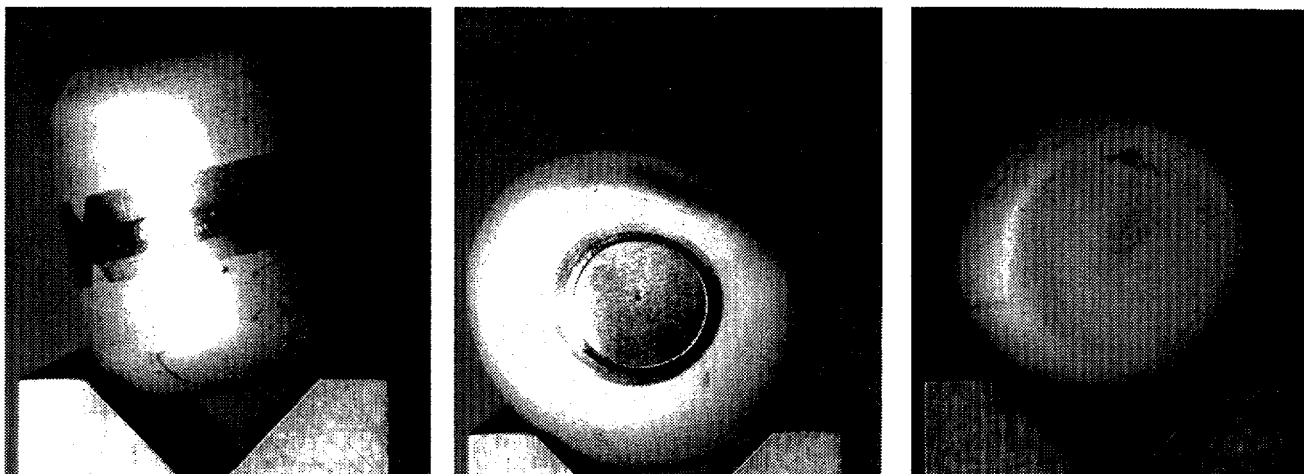
Fig. 2. HSC-1 Half module; (a) impact face, (b) 90 deg face, (c) 180 deg face, and (d) 270 deg face.  
(NMT-9 Negs. 955-75, 955-78, 955-76, 955-77)



(a)

(b)

(c)



(d)

(e)

(f)

Fig. 3. Capsule FC0007 was moderately deformed by the impact; (a) 0 deg weld location, (b) 90 deg weld location, (c) 180 deg weld location, (d) 270 deg weld location, (e) vent end, and (f) blind end. (NMT-9 Negs. 955-36, 955-37, 955-38, 955-39, 955-34, 955-35)

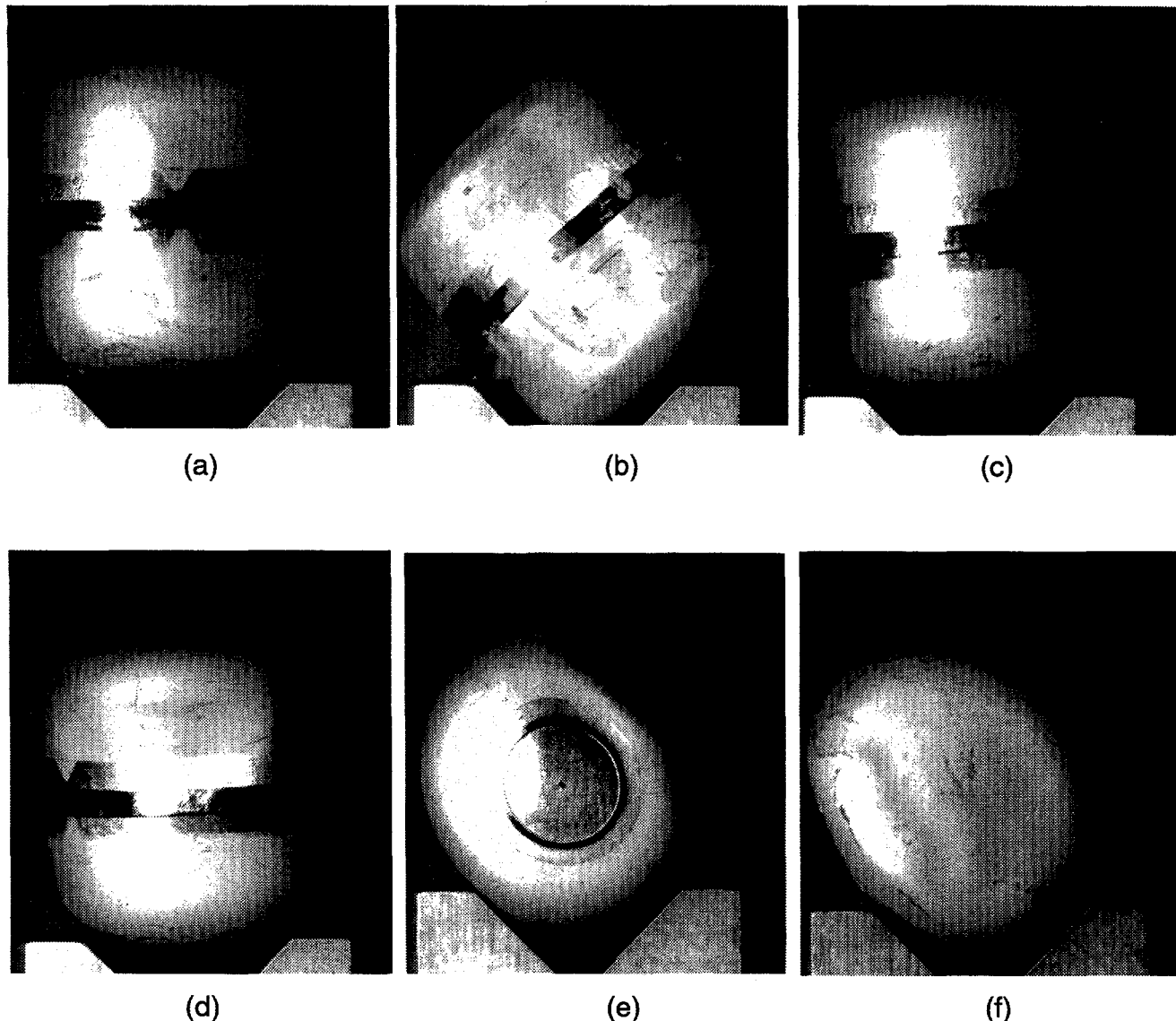
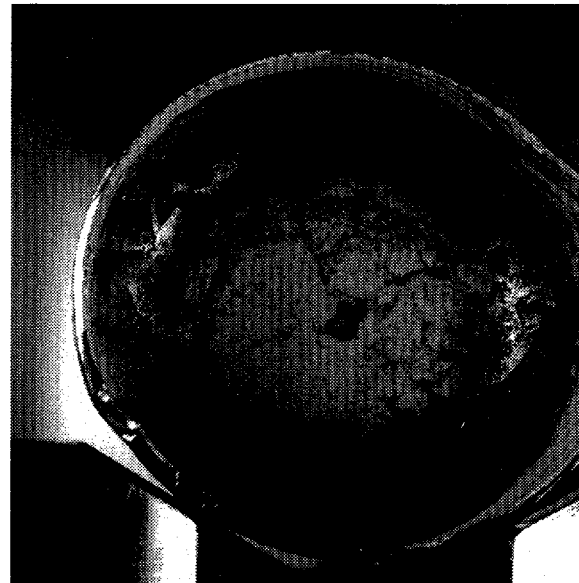


Fig. 4. Capsule FC0010 also experienced significant deformation; (a) 0 deg weld location, (b) 90 deg weld location, (c) 180 deg weld location, (d) 270 deg weld location, (e) vent end, and (f) blind end. (NMT-9 Negs. 955-42, 955-43, 955-44, 955-45, 955-40, 955-41 )

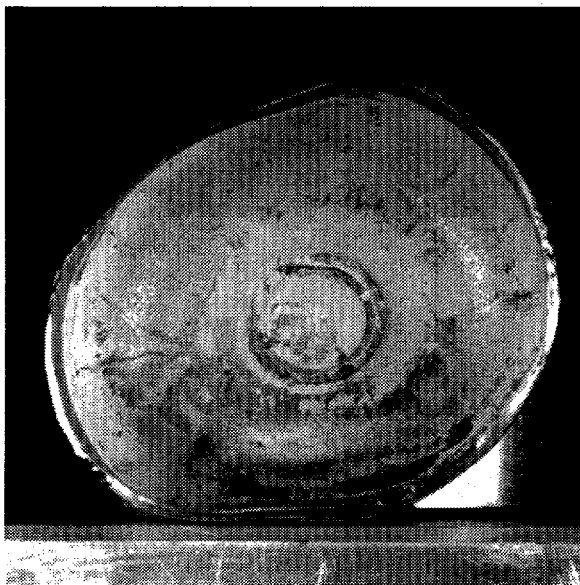


(a)



(b)

Fig. 5. A thin coating of white powder was observed on the interior of capsule FC0007; (a) vent cup, and (b) shield cup. (NMT-9 Negs. 955-46, 955-47)



(a)



(b)

Fig. 6. The interior of capsule FC0010 also had a white coating on the interior of both cups; (a) vent cup, and (b) shield cup. (NMT-9 Negs. 955-68, 955-67)

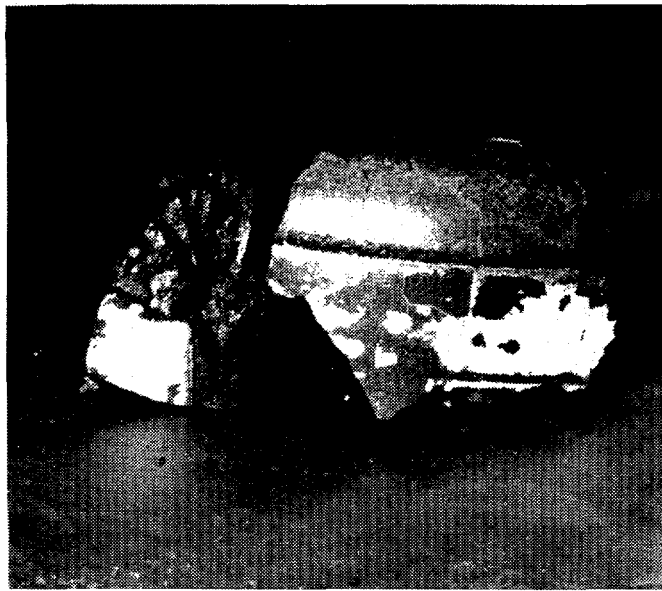
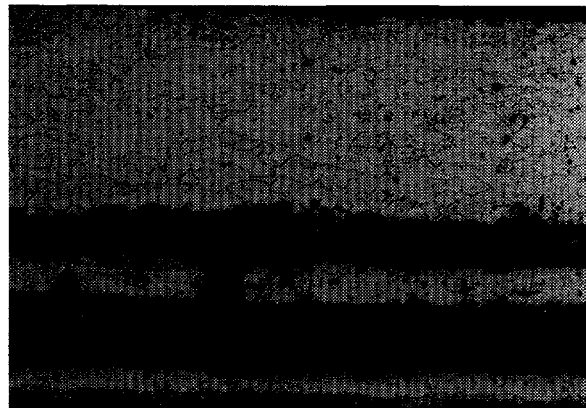


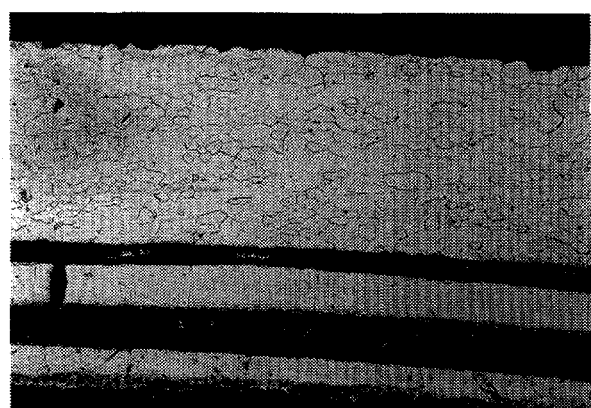
Fig. 7. The GQ-02 fuel pellet was also coated with a layer of white material.  
(NMT-9 Neg. 955-50)



Fig. 8. Breakup of the GQ-02 fuel pellet was typical of previous GPHS impacts.  
(NMT-9 Neg. 955-48)

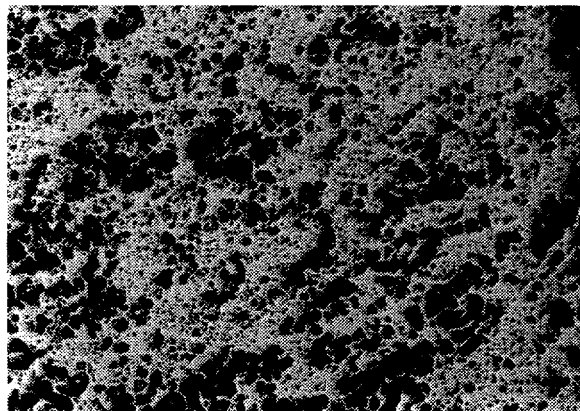


(a)

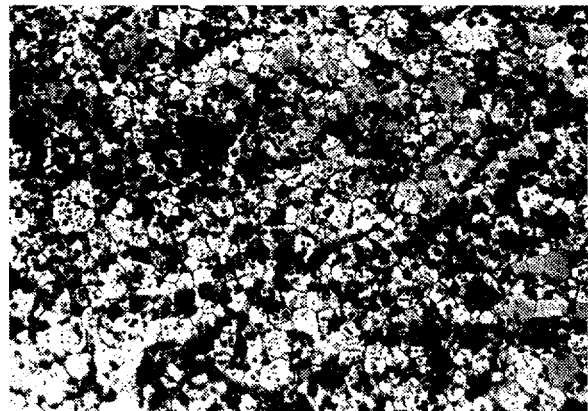


(b)

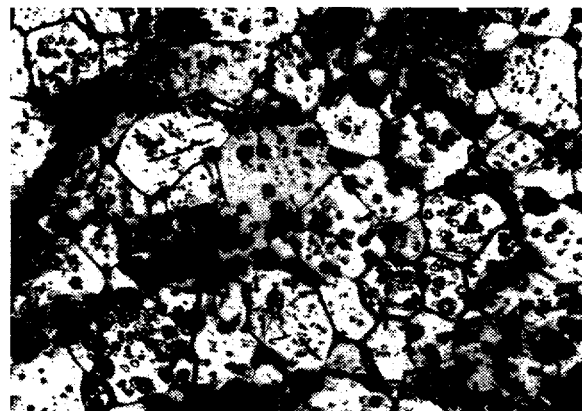
Fig. 9. The HSC-1 capsule vents were free of deposits or anomalous microstructures; (a) capsule FC0007 vent, (b) FC0010 vent, both as-etched and at 50X magnification.  
(NMT-9 Negs. 959-16, 957-94)



(a)



(b)



(c)

Fig. 10. The GQ-02 pellet microstructure appeared normal. (a) As-polished, 100X magnification; (b) etched, 100X magnification; and (c) etched, 250X magnification. (NMT-9 Negs. 959-42, 9513-90, 9513-88)

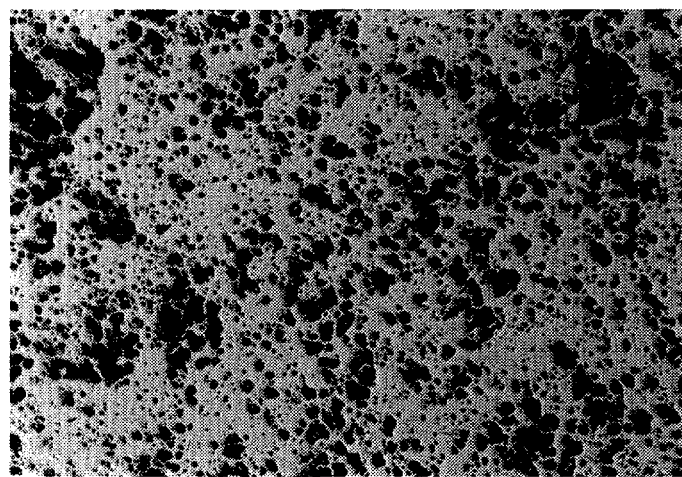
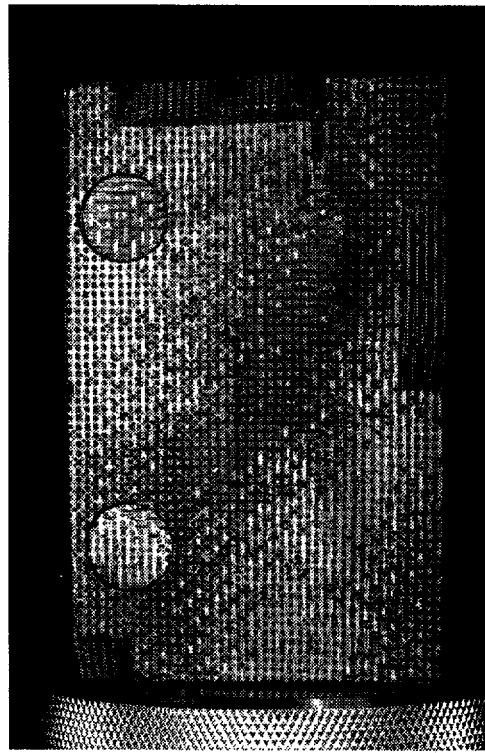
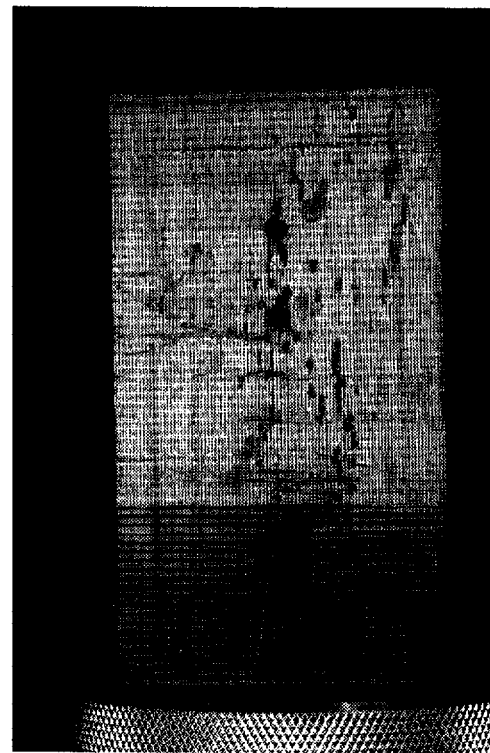


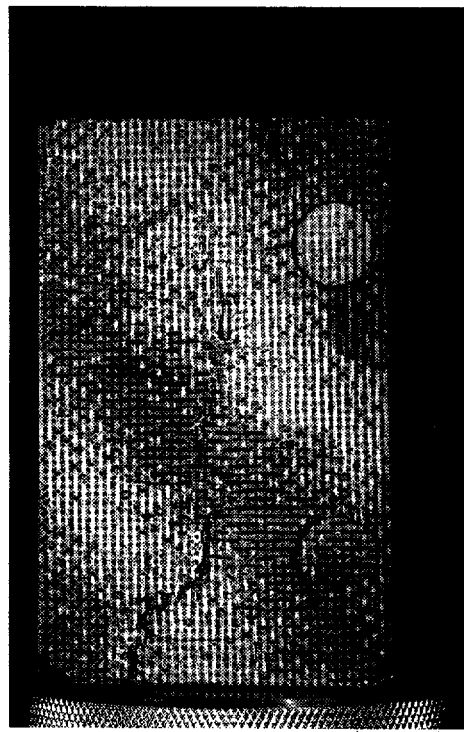
Fig. 11. The as-polished appearance of the GQ-04 fuel pellet was typical; 100X magnification. (NMT-9 Neg. 959-39)



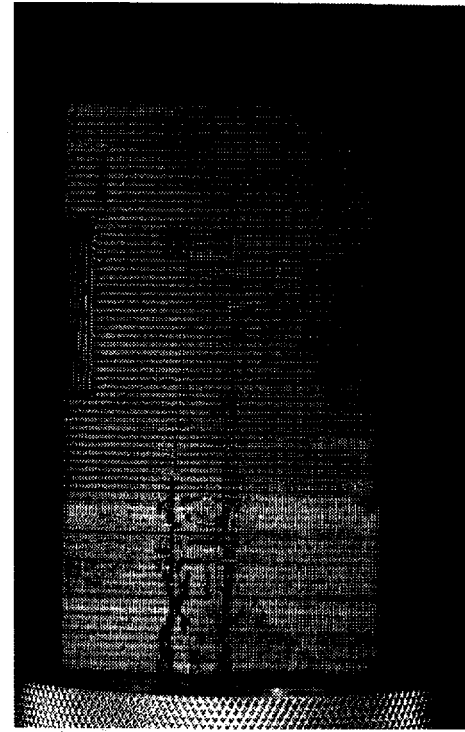
(a)



(b)

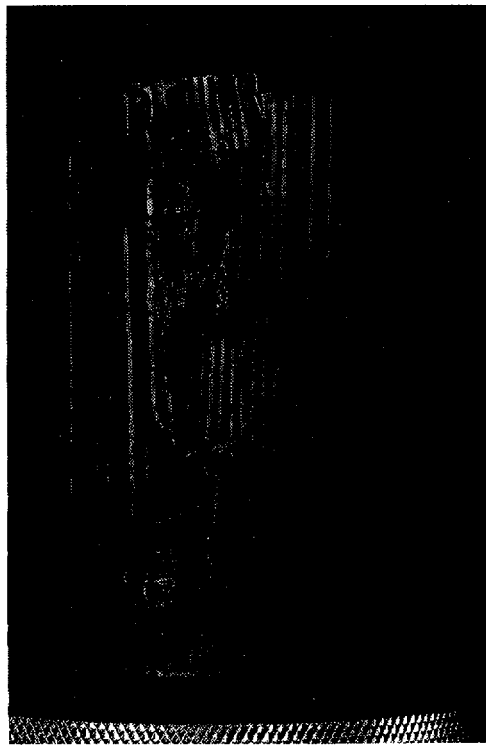


(c)

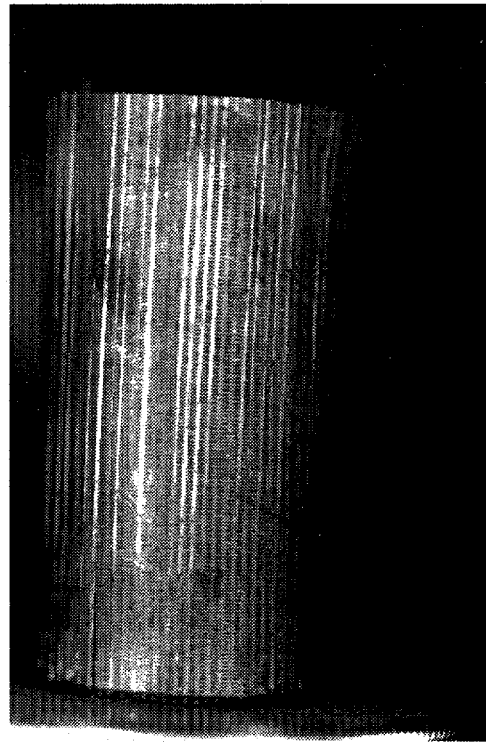


(d)

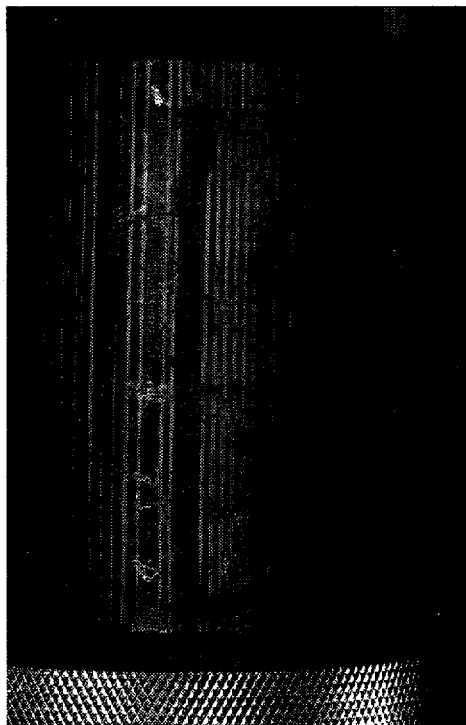
Fig. 12. HSC-2 half module; (a) impact face, (b) 90 deg face, (c) 180 deg face, and (d) 270 deg face. (NMT-9 Negs. 955-51, 955-52, 955-53, 955-54).



(a)



(b)



(c)



(d)

Fig. 13. The HSC-2 GIS was relatively intact; (a) impact face, (b) 90 deg face, (c) 180 deg face, and (d) 270 deg face. (NMT-9 Negs. 955-57, 955-61, 955-59, 955-58)

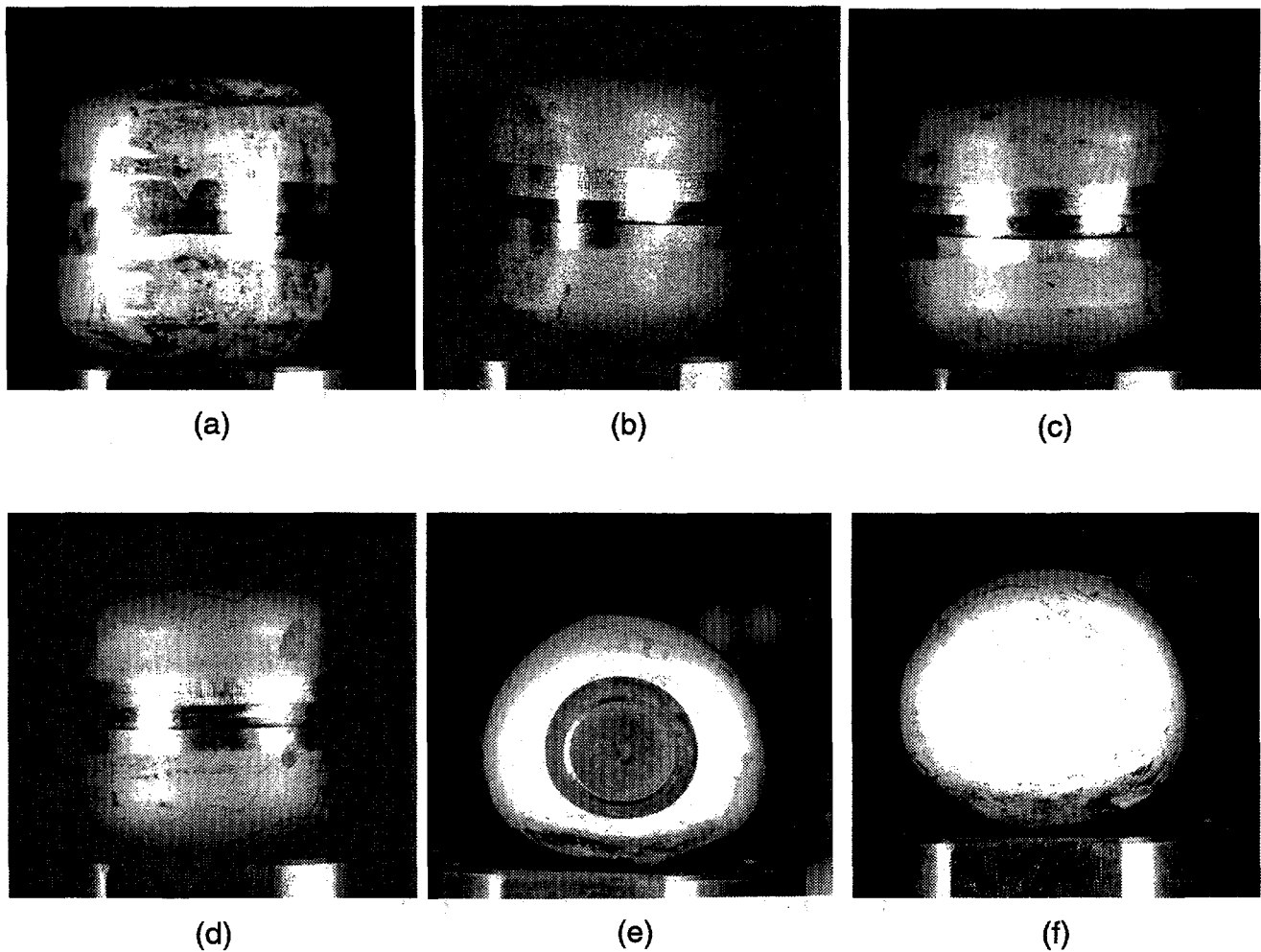


Fig. 14. Capsule FC0033 was unbreached; (a) 0 deg weld location, (b) 90 deg weld location, (c) 180 deg weld location, (d) 270 deg weld location, (e) vent end, and (f) blind end. (NMT-9 Negs. 955-74, 955-72, 955-73, 955-74, 955-69, 955-70)

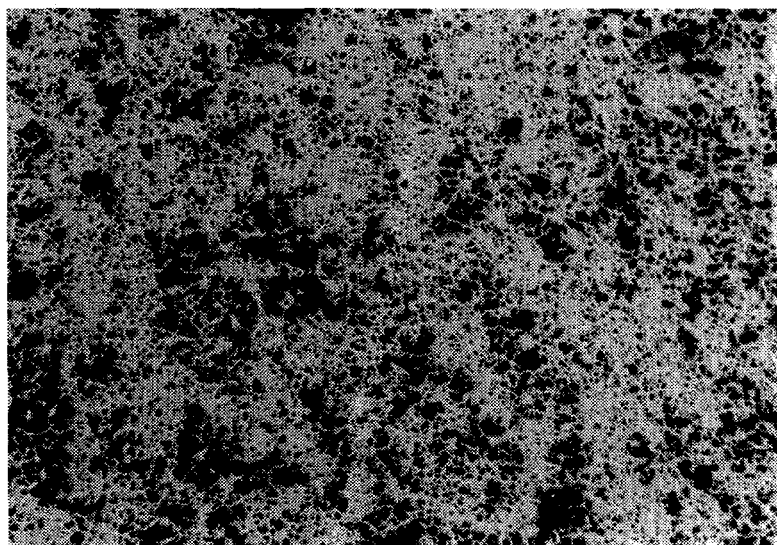


Fig. 15. The as-polished appearance of the GF-20 fuel pellet was typical; 100X magnification. (NMT-9 Neg. 959-36)

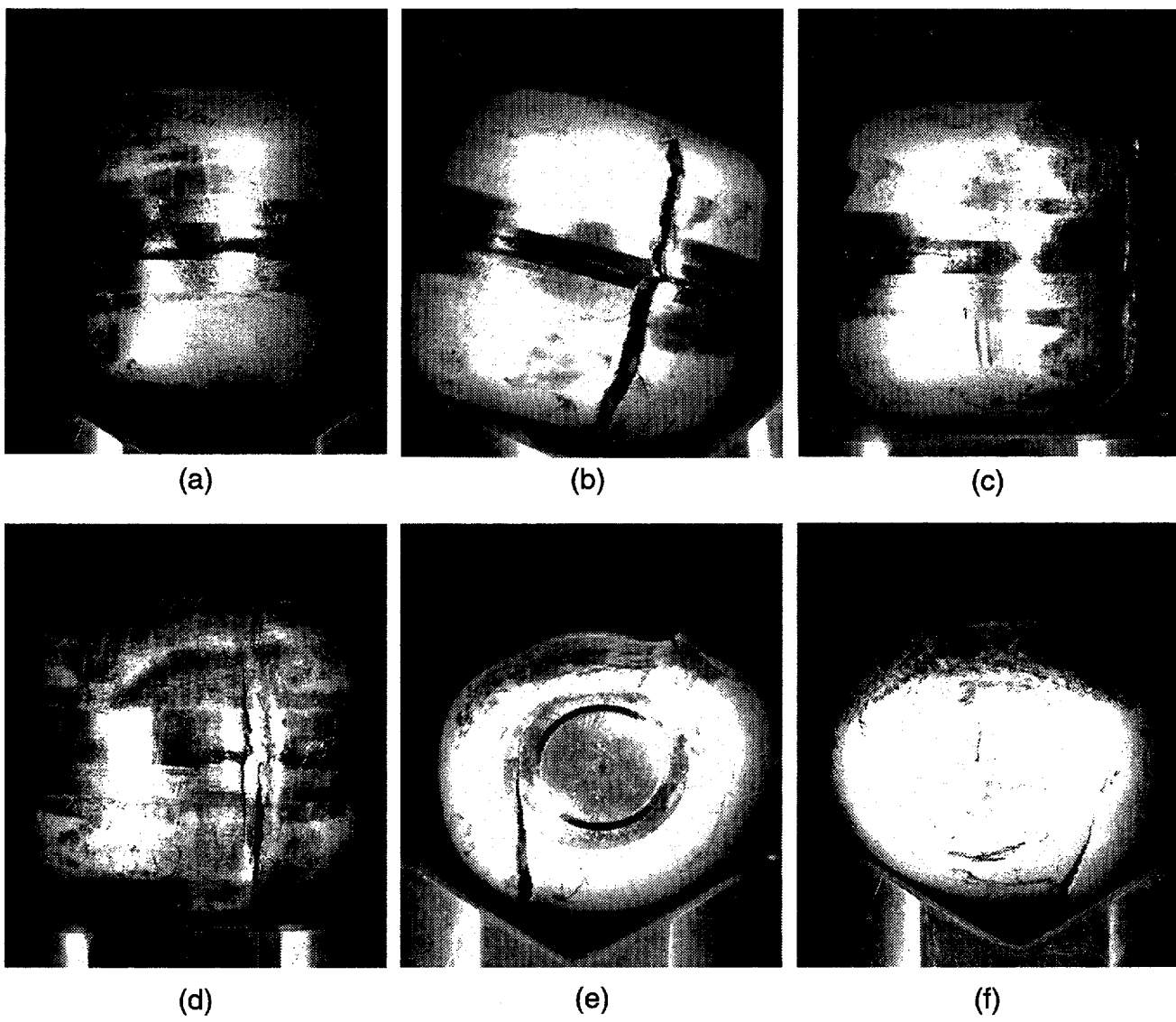


Fig. 16. Capsule FC0035 was breached by the massive differential displacement of large fuel fragments; (a) 0 deg weld location, (b) 90 deg weld location, (c) 180 deg weld location, (d) 270 deg weld location, (e) vent end, and (f) blind end. (NMT-9 Negs. 955-63, -64, -65, -66, -61, -62)

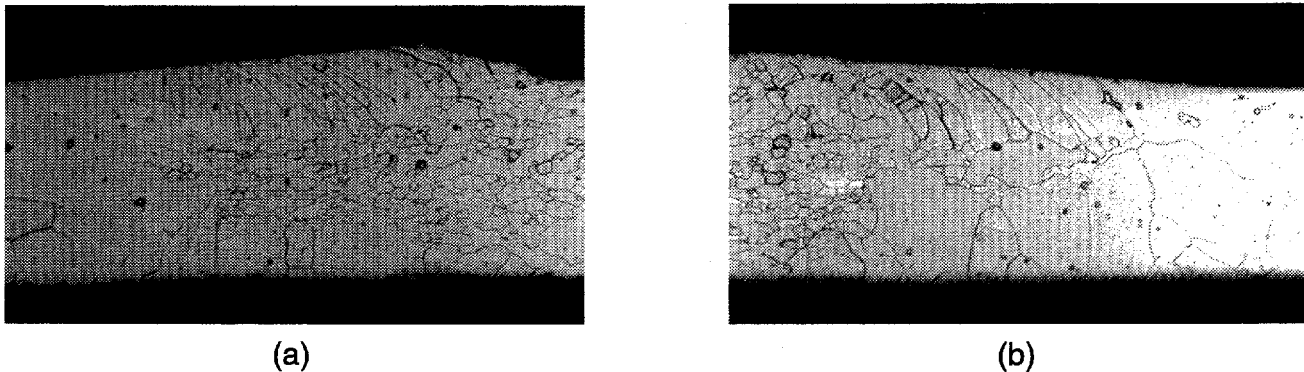
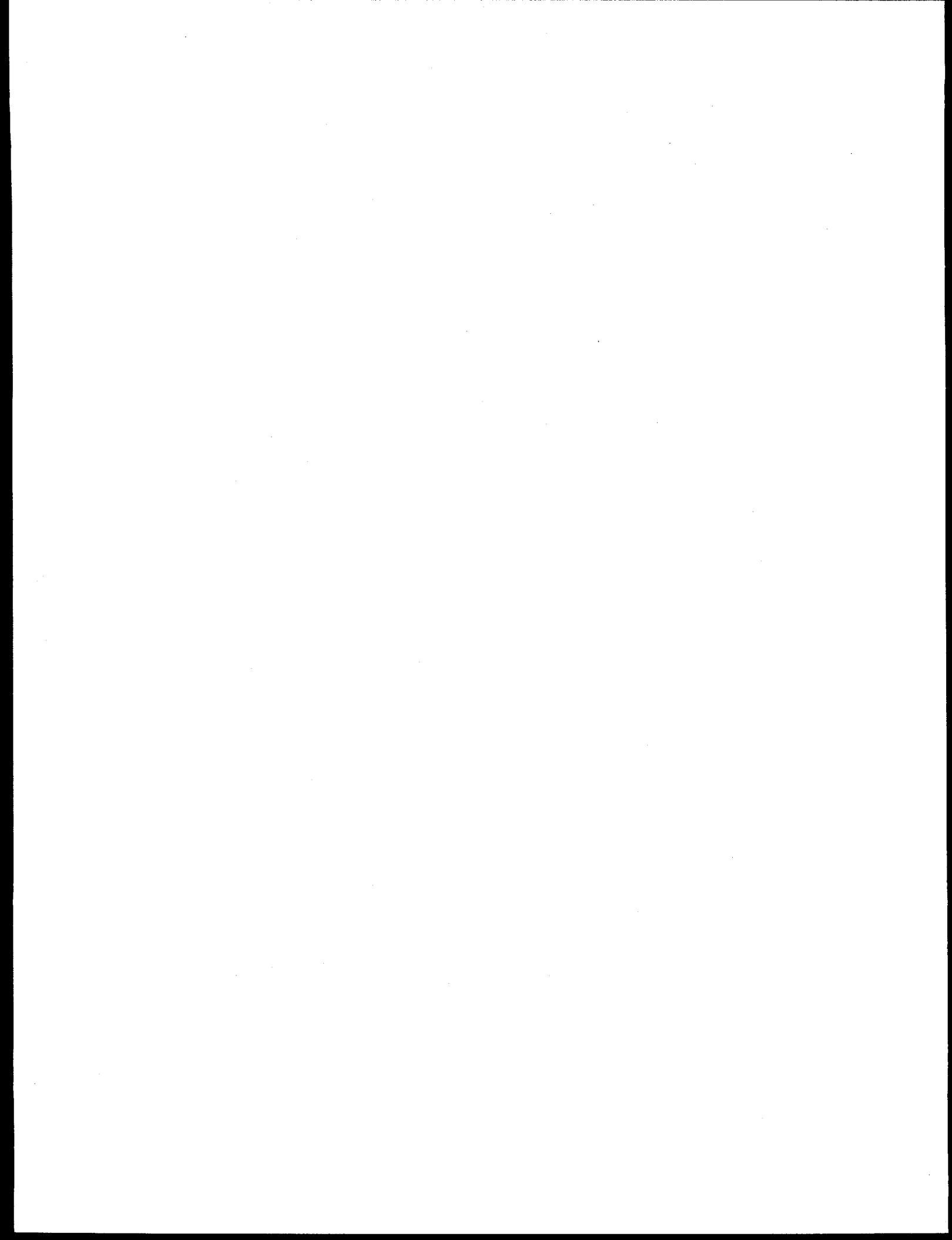


Fig. 17. Pronounced grain coarsening was observed in an FC0035 vent cup section, below and adjacent to the vent cover welds; (a) and (b), both etched and at 50X magnification. (NMT-9 Negs. 959-49, 959-50)



This report has been reproduced directly from the  
best available copy.

It is available to DOE and DOE contractors from the  
Office of Scientific and Technical Information,  
P.O. Box 62,  
Oak Ridge, TN 37831.  
Prices are available from  
(615) 576-8401.

It is available to the public from the  
National Technical Information Service,  
US Department of Commerce,  
5285 Port Royal Rd.  
Springfield, VA 22616.

**Los Alamos**  
NATIONAL LABORATORY

Los Alamos, New Mexico 87545